Available online at www.sciencedirect.com
SCIENCE DIRECT
Polymer 46 (2005) 9881–9891
polymer
www.elsevier.com/locate/polymer

Filled poly(2,6-dimethyl-1,4-phenylene oxide) dense membranes by silica and silane modified silica nanoparticles: characterization and application in pervaporation

M. Khayet[a,*], J.P.G. Villaluenga[a], J.L. Valentin[b,1], M.A. López-Manchado[b,1], J.I. Mengual[a], B. Seoane[a]

[a]*Department of Applied Physics I, Faculty of Physics, University Complutense of Madrid, Av. Complutense s/n, 28040 Madrid, Spain*
[b]*Institute of Polymer Science and Technology, C/ Juan de la Cierva, 3, 28006 Madrid, Spain*

Received 11 January 2005; received in revised form 15 June 2005; accepted 27 July 2005
Available online 11 August 2005

Abstract

The effects of silica and silane modified silica fillers on the pervaporation properties of poly(2,6-dimethyl-1,4-phenylene oxide) (PPO) dense membranes have been studied. Crystallinity, thermal and mechanical properties of unfilled and filled PPO membranes with silica and silane modified silica nanoparticles were investigated. The surface energy together with the solubility parameters of the membranes and the nanoparticles were determined. Pervaporation separation of methanol/methyl *tert* butyl ether (MTBE) mixtures over the entire range of concentration were carried out using both filled and unfilled membranes. The results are discussed in terms of the solubility and the diffusivity of each liquid component in the membranes. Flory–Huggins theory was used to predict the sorption methanol selectivity. Compared to the unfilled PPO membrane, the filled PPO membranes exhibit higher methanol selectivity and lower permeability. For methanol concentration in liquid feed mixture lower than 50 wt%, methanol selectivity of the filled PPO membranes with silane modified silica is better than that of the silica filled and unfilled PPO membranes.

Keywords: Pervaporation; Composite poly(phenylene oxide) membranes; Separation

1. Introduction

Inorganic particles have been dispersed in polymeric matrix for preparation of dense or porous composite membranes [1–8]. The obtained membranes have controllable physical properties, which are achieved by combining the properties of both organic polymers and inorganic dispersed particles. These membranes have been used in gas and liquid separation processes [1–8]. Various types of inorganic fillers have been dispersed in different polymer matrixes [1–8]. In this study, poly(phenylene oxide), PPO has been used as substrate for preparation of dense filled membranes by silica and silane modified silica nanoparticles, because of its low separation performance in pervaporation and gas separation [9–12].

PPO has been modified by various methods including bromination, sulfonation, nitration, and carboxylation, to improve its selectivity [9]. Thin film composite PPO and modified PPO membranes have been applied in liquid separation such as reverse osmosis, pervaporation and nanofiltration and in gas separation [9–12]. In the present study, permeation experiments using unfilled PPO and filled PPO membranes with silica and silane modified silica nanoparticles were conducted using the separation process pervaporation (PV). In this process, a liquid mixture is brought in direct contact with the feed side of the membrane and the permeate is removed as vapor from the other side of the membrane. The mass flux is driven by maintaining the downstream partial pressure lower than the saturation pressure of the liquid feed solution. In PV, the transport of liquids through the membranes differs from other membrane processes using dense membranes such as gas separation,

* Corresponding author. Tel./fax: +34 91 3945191.
E-mail address: khayetm@fis.ucm.es (M. Khayet).
[1] Tel.: +34 91 5622900; fax: +34 91 5644853.

0032-3861/$ - see front matter © 2005 Elsevier Ltd. All rights reserved.
doi:10.1016/j.polymer.2005.07.081

because the permeants in PV usually show high solubility in polymeric membranes.

Among the various liquid mixtures used, methanol/-methyl *tert* butyl ether (MTBE) is one of the most interesting and important mixtures to be separated by PV. MTBE has gained great attention as a gasoline additive, octane enhancer, to replace lead additives. The octane enhancers increase the octane index of gasoline and are excellent oxygenated fuel additives that decrease carbon monoxide emissions. For this reason, the production of MTBE has been increased dramatically during the last years. MTBE is produced by the reaction of methanol and isobutylene (2-methyl-1-propene) in the liquid phase over a strongly acidic ion exchange resin catalyst. It is often desired to add methanol in up to 20% to improve the reaction conversion. However, the use of excess methanol causes a purification problem because methanol forms an azeotrope with MTBE, which is difficult to separate by distillation. PV, which is a more energy efficient and lower cost process, has been used to break this azeotrope using a series of polymeric and inorganic membranes [13–22].

The objective of this study is to investigate the PV performance of filled PPO membranes with silica and silane modified silica nanoparticles to separate methanol/MTBE mixtures. The prepared membranes were first characterized by different physical techniques. Swelling experiments and PV separation of methanol from its mixture with MTBE over the entire range of concentration, 0–100%, were carried out.

2. Experimental

2.1. Materials

Poly(2,6-dimethyl-1,4-phenylene oxide) (PPO) powder of intrinsic viscosity 1.57 dl/g in chloroform at 25 °C, and density 1.04 g/cm^3 was supplied by General Electric (GE). Analytical grade (AR) chloroform was purchased from Aldrich Chemicals and used as solvent for the preparation of the membranes. The silica nanoparticle used in this study is Ultrasil VN3 provided by Degussa Hüls AG (Frankfurt, Germany). The silane used for modification of the silica nanoparticle is bis(triethoxysilylpropyl) tetrasulfane (Si69) manufactured by Degussa Hüls AG (Bitterfeld, Germany). Toluene (Merck, 99.9%), diethyl oxide (Panreac Química S.A.) and petroleum ether 40–60 °C (Panreac Química S.A.) were used to conduct silanization reaction. Methanol (MeOH, Panreac Química S.A., 99.8%) and methyl *tert* butyl ether (MTBE, Panreac Química S.A., 99%) were employed in pervaporation experiments.

2.2. Silanization reaction

Silane modified silica nanoparticles were prepared using the following reaction: 25 g of silica was first added into 150 ml of toluene and then 7.5 g of silane was poured into the solution under vigorous stirring for a period of 6 h at a temperature of 80 °C. Fig. 1 shows a schematic representation of the silanization mechanism. The precipitated was collected on a clock filter and washed with diethyl oxide and petroleum ether until no silane was detected. Finally, the samples were dried at 70 °C for 8 h in vacuum.

The surface modification of silica with the organosilane reduces the number of the superficial silanol groups, and grafts molecules with an organic nature. A couple of reactions will take place: (1) between the silanol groups of the silica and the triethoxysilyl groups of the silane via hydrolysis with loss of ethanol, and (2) condensation reactions and crosslinking between pairs of neighboring silane molecules, which are already bound to the silica surface.

2.3. Characterization of modified and unmodified silica nanoparticles

2.3.1. Environmental scanning electron microscopy (ESEM)

The distribution of the superficial silanization of silica nanoparticles was studied by environmental scanning electron microscopy (ESEM) using a Philips XL30 under a 15 kV voltage, 2 °C temperature and 5 Torr pressure. In this case, solid compact disk samples of both unmodified and modified nanoparticles were prepared by applying a pressure of about 10 tons over a cylindrical ring filled with these nanoparticles. The micro-drops formed on the sample will give information not only about the proportion of organo-modification, but also about the distribution of the grafted molecules on the surface of the silica.

2.3.2. Surface area measurement

Nitrogen adsorption isotherms were obtained at 77 K using a static volumetric Micromeritics Gemini 2360 apparatus. The samples were first degassed, at 140 °C, for about 12 h in a Micromeritics FlowPrep 060. To determine the surface area of the unmodified silica and silane modified nanoparticles, the molecular cross section of nitrogen used in the BET data analysis was 16.2 Å^2.

2.3.3. Contact angle measurement:

Advancing contact angles of both unmodified and modified silica disk samples were measured at 25 °C on an optical contact angle meter CAM 200 equipped with a CCD camera, frame grabber and image analysis software. Distilled water (W), ethylene glycol (ETG, Normapur™ AR, 99.7% purity) and diiodomethane (DIM, Aldrich, 99% purity) were used. Contact angles were obtained by placing the tip of the syringe near the sample surface and depressing the syringe to produce a constant drop volume of about 2 μl. Five to six drops per sample and 20 reading per each drop were carried out with 1 s settling time. For each sample, the

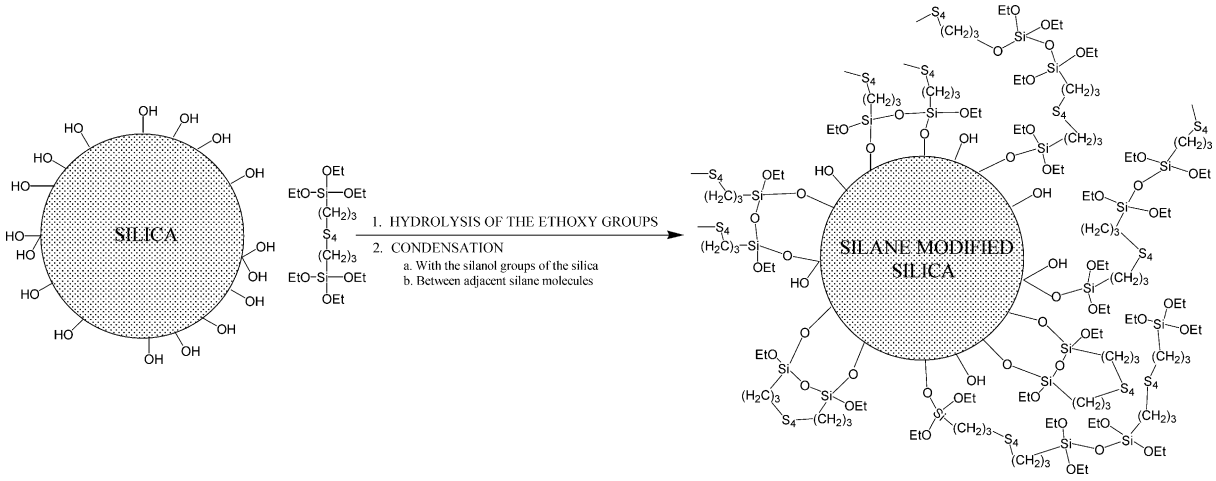

Fig. 1. Schematic representation of the silanization mechanism of the silica nanoparticle (S4 refers to the tetrasulfane group).

average value together with their standard deviation were calculated and reported in this study.

2.4. Membrane preparation

The method used for preparation of PPO membranes was similar to that described in detail elsewhere [11,12]. In this study, the PPO content in chloroform is 4 wt% and the used concentration of silica and silane modified silica nanoparticles in the polymer solution is 5 and 10 wt%. The so prepared membranes are named hereafter PPO for the unfilled membrane, SPPO1 and SPPO2 for the filled PPO membranes with 5 and 10 wt% unmodified silica, respectively; and MSPPO1 and MSPPO2 for the filled PPO membranes with 5 and 10 wt% silane modified silica nanoparticle, respectively.

The thicknesses of the membranes, measured by a Millitron micrometer (Mahr Feinpruf, type 1202 IC), were: 49.1 ± 2.2, 50.8 ± 3.2, 47.4 ± 3.2, 48.9 ± 3.4 and 51.7 ± 3.7 μm for the membranes PPO, SPPO1, SPPO2, MSPPO1 and MSPPO2, respectively.

2.5. Membrane characterization

2.5.1. Contact angle measurements

The procedure used for contact angle measurements of the membranes is similar to that mentioned previously. The contact angles of the three liquids distilled water (W), ethylene glycol (ETG) and diiodomethane (DIM) are also measured.

2.5.2. X-ray diffraction

X-ray diffraction spectra of both filled and unfilled membranes were obtained using a Philips PW 1830 X-ray diffractometer. The diffractograms were measured at 2θ in the range of 2–40° using Cu K_α radiation ($\lambda = 1.54$ Å) monochromated by means of a nickel filter, a tube voltage of 40 kV and tube current of 25 mA.

2.5.3. Thermal gravimetric analysis (TGA)

Thermal degradation measurements of the membrane samples were performed using a Mettler Toledo thermogravimetric analyzer (TGA, model SDTA 851). Temperature programs were run from 30 to 600 °C at a heating rate of 10 °C/min. Nitrogen flow of 20 ml/min was utilized in order to remove all corrosive gas involved in the degradation and to avoid thermoxidative degradation.

2.5.4. Mechanical tests

Tensile testing was performed at room temperature on an Instrom dynamometer model 4301, according to ASTM D 638M (standards). Tests were carried out with a crosshead speed of 50 ml/min at break. At least five measurements were performed for each membrane sample and the average values are reported in this study.

2.5.5. Swelling measurements

Dry membrane samples were first weighted and then immersed in MeOH, MTBE or in a mixture of these solvents of various concentrations. The samples were allowed to equilibrate for more than 72 h at a temperature of approximately 25 °C. Swollen membranes were taken out from the solutions, wiped carefully with filter paper and weighted again. Finally, the overall solubility was calculated from the weight of the swollen and the dry membrane sample according to the following expression.

$$S = \frac{m_W - m_D}{m_D} \quad (1)$$

where m_W and m_D are the masses of the swollen and dry membrane, respectively.

2.5.6. Pervaporation experiments

The experimental pervaporation apparatus used in this study was described in a previous paper [23]. The membrane is installed in the stainless steel pervaporation cell equipped with a heating jacket and the feed liquid

containing MeOH, MTBE or a mixture of both was circulated through the pervaporation cell, in a direct contact with the feed side of the membrane. The feed reservoir was maintained at a temperature of 25 °C. The pressure at the downstream side was kept at approximately 1 mm Hg by means of a vacuum pump. The permeate fluxes were determined by measuring the weight of the liquid collected in the cold traps cooled by liquid nitrogen during a certain time, at steady-state conditions. The feed and permeate compositions were analyzed at approximately 25 °C by measuring the refractive indexes with an Abbey-type refractometer Model 60/ED (Bellingham + Stanley Ltd).

3. Results and discussion

3.1. Characteristics of unmodified and silane modified silica nanoparticles

As stated earlier both modified and unmodified silica nanoparticles were characterized by means of contact angle measurements, nitrogen adsorption and ESEM technique. The results are given in Table 1 and in Fig. 2. It can be observed differences in contact angles (Table 1), surface area and water drop distribution (Fig. 2) between the unmodified and the silane modified silica samples. The silane modified silica are more hydrophobic than the unmodified silica (i.e. water contact angle of the unmodified silica is found to be 30.4° while that of the silane modified silica is higher, 67.5°), and the surface area of the silica nanoparticles decreases from 164 m^2/g for the unmodified silica to 72 m^2/g for the silane modified silica. These facts confirm the surface modification by silanization reaction (Fig. 1), which reduces the number of superficial silanol groups, and grafts molecules with organic nature forming silane stable network on silica surface. Thus, the hydrophilic inorganic silica nanoparticle is surface modified to a hydrophobic organic–inorganic nanoparticle.

ESEM technique permits the direct visualization of micrometric water drop distribution over the top surface of the samples without further metal coating. Fig. 2(a) and (b) shows the ESEM images of the unmodified silica and the silane modified silica, respectively. A difference in shape, volume and distribution of water drops formed over each sample can be detected. This also demonstrates the surface changes on the silica by silanization reaction. Unmodified silica sample (Fig. 2(a)) shows different shapes and volumes of water drops. This is due to the fact that water spread more easily over this surface and irregular forms of water drops

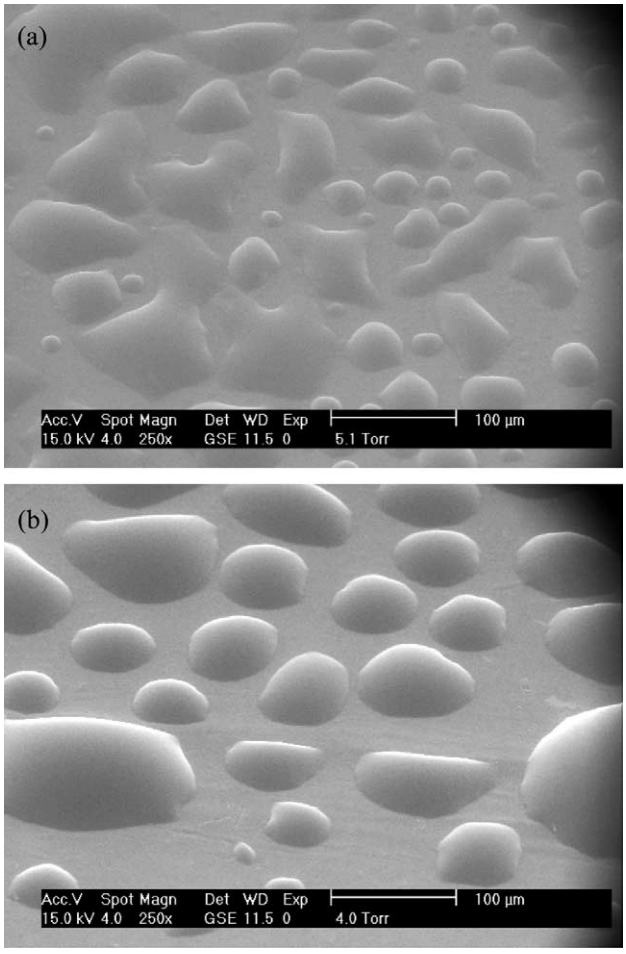

Fig. 2. ESEM images of water drops formed on disk samples of the unmodified silica (a) and the silane modified silica (b).

Table 1
Contact angles (water, θ_W, ethylene glycol, θ_{ETG}, diiodomethane, θ_{DIM}), surface energy components, cohesive energy density (e_{coh}) and solubility parameter (δ) of unmodified silica, silane modified silica, unfilled PPO and filled PPO membranes (SPPO1, SPPO2, MSPPO1, MSPPO2)

Membrane	PPO	SPPO1	SPPO2	MSPPO1	MSPPO2	Umodified silica	Modified silica
θ_W (°)	88.3±2.0	83.9±1.8	81.9±2.3	86.4±2.5	84.0±2.1	30.4±1.9	67.5±2.1
θ_{ETG} (°)	69.6±0.9	58.2±1.8	51.9±2.8	50.46±1.1	51.0±2.2	21.3±1.7	47.1±1.9
θ_{DIM} (°)	47.6±1.9	43.3±2.4	43.2±1.9	41.4±2.5	37.3±2.0	38.4±2.0	41.2±2.2
γ_s^{LW} (mJ/m^2)	35.58	37.92	37.95	38.91	40.97	40.41	39.00
γ_s^{AB} (mJ/m^2)	2.07	0.26	1.67	1.50	1.13	4.42	1.32
γ_s^{+} (mJ/m^2)	0.19	0.003	0.15	0.31	0.11	0.09	0.03
γ_s^{-} (mJ/m^2)	5.50	4.92	4.57	1.80	2.91	52.46	16.23
γ_s^{total} (mJ/m^2)	37.65	38.19	39.62	40.41	42.10	44.83	40.32
e_{coh} (10^6 J/m^3)	355.69	363.30	383.92	395.45	420.61	462.12	394.21
δ (10^3 J$^{1/2}$/m$^{3/2}$)	18.86	19.06	19.59	19.89	20.51	21.50	19.85

appear, indicating greater affinity of silica to water, and minor contact angles are expected. In contrast, in Fig. 2(b), a more homogenous surface with almost spherical and regular water drops can be observed suggesting higher cohesion force than adhesion one. In other words, water drops show a weak interaction with the silane modified silica surface indicating higher water contact angle than the unmodified silica. These observations are in line with the corresponding contact angle values summarized in Table 1. More explanation related with the compatibility of these nanoparticles with PPO polymer will be discussed later on.

3.2. Physical and mechanical characterization of the membranes

The crystallinity, the thermal and the mechanical properties of both unfilled and silica filled PPO membranes were studied by means of the physical techniques outlined previously. According to Wijmans et al. [24], PPO is a semicrystalline polymer and contains a very low crystalline content after membrane formation. This statement is in accordance with the obtained X-ray diffraction (XRD) spectra of all membranes tested in this study. Furthermore, it is generally believed that the unit cell of PPO crystallization changes according to the solvent used and the membrane preparation conditions [25]. In this study, both filled and unfilled PPO membranes exhibit five broad peaks in the XRD spectra. The diffraction angles together with the corresponding *d*-spacings are summarized in Table 2 for each membrane. Almost no change in *d*-spacing can be observed between the unfilled and the filled PPO membranes. Moreover, it is obvious that the membrane samples examined have very small particle sizes because of their broad peaks. From Table 2, it may be stated that the incorporation of unmodified and modified silica hardly varies the crystalline structure of PPO. In addition, following the statement described by Khulbe et al. [25], the peaks *d*3 (110) and *d*4 (200) can lead to an orthorhombic model for packing of macromolecules in the *a*–*b* plane, while *d*5 (211) will give a value of the repeat distance of two monomers in zigzag along the *c*-axis. The parameters of the packing of PPO chain molecules were determined by application of crystallographic formulae for interplanar spacings of the orthorhombic crystal system. The results, also summarized in Table 2, were found in accordance with those reported by Khulbe et al. [25].

The thermal decomposition expressed in terms of weight loss as a function of the temperature for the unfilled and the filled PPO membranes is reported in Table 3. The decomposition of all membranes is characterized in only one step with approximately a 70% loss weight. It is of interest to note that a higher thermal stability is attained for the filled PPO membranes, which exhibit higher decomposition temperature than the unfilled PPO membrane. That is, the incorporation of modified and unmodified silica shows an enhancement of the thermal stability of PPO membrane.

Table 2
Parameters for diffraction peaks from unfilled PPO and filled PPO membranes with silica and silane modified silica nanoparticles

Membrane	$2\theta_1$	d_1 (Å)	$2\theta_2$	d_2 (Å)	$2\theta_3$	d_3 (Å)	$2\theta_4$	d_4 (Å)	$2\theta_5$	d_5 (Å)	$\vec{a}$ (Å)	$\vec{b}$ (Å)	$\vec{c}$ (Å)
PPO	5.37	16.44	8.02	11.01	13.12	6.74	16.69	5.31	21.30	4.17	10.61	8.73	10.63
SPPO1	5.18	17.04	8.09	10.92	13.19	6.70	16.43	5.39	21.72	4.09	10.78	8.55	9.25
SPPO2	5.24	16.84	8.02	11.01	13.12	6.74	16.63	5.32	21.53	4.12	10.64	8.71	9.81
MSPPO1	5.44	16.23	8.15	10.84	12.99	6.81	16.76	5.28	21.33	4.16	10.56	8.91	10.35
MSPPO2	5.38	16.41	8.09	10.92	13.32	6.64	16.96	5.22	21.99	4.04	10.44	8.60	9.51

Table 3
Thermal properties of the unfilled and the filled PPO membranes with the unmodified silica and the silane modified silica nanoparticles

Membrane	Decomposition temperature (°C)	Carbonaceous residues (%)
PPO	446±1.0	29.9±0.1
SPPO1	454±1.0	31.8±0.1
SPPO2	454±1.0	35.3±0.1
MSPPO1	454±1.0	31.0±0.1
MSPPO2	454±1.0	35.1±0.1

The mechanical properties of the membranes are summarized in Table 4. The tensile properties are given in terms of Young's modulus, maximum strength and the percent elongation at break. It can be seen that the addition of the unmodified and the silane modified silica hardly affects the mechanical properties of dense PPO membranes, since the amount of filler used in the preparation of the membranes is relatively low and PPO membrane itself possesses excellent mechanical properties.

3.3. Contact angle analysis

Table 1 shows the distilled water (W), ethylene glycol (ETG) and diiodomethane (DIM) contact angles of unfilled and filled PPO membranes together with their standard errors. For all membranes the contact angle values are higher for water, followed by those of ethylene glycol and then those of diiodomethane. It can be observed that, for the three liquids used, the contact angle of PPO membranes are higher than those of the filled PPO membranes. Because the contact angles of the polar liquid water is quite high on all membranes, the contact angle of water do not appear to be significantly affected by the addition of silica and modified silica nanoparticles in PPO membranes.

The surface energy components of the membranes were determined from contact angle measurements using the Lifshitz-van der Waals (LW) method also known as acid–base (AB) approach or van Oss, Good, and Chaudhury method [26,27]. The theory behind this method of estimating the solid surface free energy and its components has been extensively described in the literature. van Oss et al. [26,27] divided the surface tension into different components, i.e. the Lifshitz-van der Waals (LW), acid (+) and base (−) components.

Table 4
Mechanical properties of the unfilled and the filled PPO membranes with the unmodified silica and the silane modified silica nanoparticles

Membrane	Young's modulus (MPa)	Maximum strength (MPa)	Deformation at break (%)
PPO	2524±87	48±3	17.1±0.9
SPPO1	2595±93	52±3	5.1±0.6
SPPO2	2608±92	52±4	4.9±0.5
MSPPO1	2470±85	48±3	8.7±0.7
MSPPO2	2502±88	48±3	8.5±0.6

$$\gamma_i = \gamma_i^{LW} + \gamma_i^{AB} = \gamma_i^{LW} + 2\sqrt{\gamma_i^+ \gamma_i^-} \quad (2)$$

where i denotes either the solid or the liquid phase. The acid–base component (γ_i^{AB}) takes into account the electron-donor (γ_i^-) and the electron-acceptor (γ_i^+) interactions. The following expression was given for solid–liquid systems [26,27].

$$(1+\cos\theta)\gamma_l = 2(\gamma_s^{LW}\gamma_l^{LW})^{1/2} + 2(\gamma_s^+\gamma_l^-)^{1/2} + 2(\gamma_s^-\gamma_l^+)^{1/2} \quad (3)$$

where the three components of the surface free energy of the solid, γ_s^{LW}, γ_s^+ and γ_s^- can be determined from the contact angle measurements of three testing liquids with known surface tension components.

The calculated surface energy components and the total surface energies are also presented in Table 1. The contact angles of diiodomethane, for which the LW components of the surface energy dominates, are different on PPO and filled PPO membranes. It can be seen that the LW surface energy component of PPO membrane is lower than those of the filled membranes, whereas the AB surface energy component of PPO membrane is higher. This is mostly due to the electron-donor (γ_s^-) contribution, which is greater for PPO membrane. For all membranes, γ_s^- is higher than γ_s^+. Moreover, γ_s^- is lower for the filled PPO membranes with silane modified silica than with the unmodified silica filled PPO membranes and unfilled PPO membrane.

A significant decrease in γ_s^- was detected with silanization reaction of silica nanoparticles. This may be due to the fact that the triethoxysilyl groups of the silane react with silanol groups present on the silica surface and to the crosslinking between neighboring silane molecules. This forms a more stable network of silane on silica surface and leads to an increase in the contact angles of the three liquids used in this study. Silica was modified with organosilanes to change the inorganic and hydrophilic nature of the silica into organic and hydrophobic nanoparticle. Furthermore, the modification of silica with silane groups decreases both γ_s^+ and γ_s^- parameters of the surface tension. Hence, other than the hydrophobicity, the polarity of silica surface is decreased by silanization reaction.

For all tested membranes, the AB surface energy component is relatively small compared to the LW surface energy component. This was observed also for unmodified silica and silane modified silica nanoparticles. It must be stated that the total surface energy of PPO is low compared to that of the filled membranes. As can be seen in Table 1, both the LW and the total surface energy show the following order: PPO < SPPO1 < SPPO2 < MSPPO1 < MSPPO2. In other words, the filled PPO membranes with silane modified silica nanoparticles exhibit higher total surface energy than the unfilled and silica filled PPO membranes.

In addition, the solubility parameter, δ, of the membranes and the nanoparticles was calculated from the following

relation [28].

$$\delta = (e_{coh})^{1/2} \quad (4)$$

where e_{coh} is the cohesive energy density, which was related to the surface free energy, γ_s, as follows.

$$e_{coh} = \left(\frac{\gamma_s}{0.75}\right)^{2/3} \quad (5)$$

where e_{coh} is in 10^6 J/m^3 and γ_s is in mJ/m^2.

The estimated values of e_{coh} and δ are also displayed in Table 1. Both e_{coh} and δ increase in the following order, PPO < SPPO1 < SPPO2 < MSPPO1 < MSPPO2. The solubility parameter of MeOH is 29.7 mJ/m^2. Therefore, from the solubility parameter approach, it is expected that the swelling degree (i.e. total equilibrium sorption) toward MeOH should be higher for the filled PPO membranes with silane modified silica nanoparticles, followed by silica filled PPO membranes and then unfilled PPO membrane [29].

It is worth quoting that the cohesive energy density and the solubility parameter of the unmodified silica is greater than that of the silane modified silica nanoparticles, which is closer to the solubility parameter of PPO polymer. Based on the solubility parameter approach [29], the solubility parameter difference, $\Delta\delta$, between each nanoparticle and PPO is found to be lower (0.99) for the silane modified silica nanoparticle than for the unmodified silica nanoparticle (2.64). This indicates that silane modified silica nanoparticles have stronger affinity and enhanced compatibility with PPO polymer than the unmodified silica nanoparticles suggesting that the silane modified silica nanoparticles will be better dispersed in PPO polymer matrix.

3.4. Sorption

According to the solution–diffusion theory, mass transport in pervaporation consists of sorption of the permeants at the liquid side of the membrane, diffusion of these permeants through the membrane and desorption at the low pressure side of the membrane. Sorption in pervaporation produces membrane swelling and causes loosening of the polymer matrix facilitating diffusion of the permeants. The overall solubility was determined as stated in Section 2.5.5. Table 5 shows the overall solubility of MeOH/MTBE mixtures in PPO and filled PPO membranes at 25 °C in all range of concentration mixture. When pure liquids are considered, both MeOH and MTBE are sorbed by the membranes and MTBE sorption is lower than that of MeOH, for all the membranes tested. In other words, MeOH is sorbed more preferentially than MTBE by PPO and filled PPO membranes. By using the solubility parameter of the membranes determined previously (Table 5), when pure MeOH is considered, solubility parameter difference, $\Delta\delta$, between each membrane and MeOH follows the same order observed previously in swelling experiments: MSPPO2 < MSPPO1 < SPPO2 < SPPO1 < PPO. That is, the swelling degree toward MeOH is higher for the membranes showing a solubility parameter close to MeOH. Furthermore, from Table 5, it can be seen that, for each membrane, the total equilibrium sorption increases with the MeOH content in the liquid mixture. On the contrary, when pure MTBE is considered, no clear tendency in the overall solubility can be observed for the different membranes. This may be attributed to the fact that sorption of a solvent not only depends on polarity and solubility parameters, but also on the free volume of the membrane, the extent of amorphous regions available in the membrane, the mutual interaction between the molecules of the mixture and the size of the penetrants [29]. MTBE is much greater than MeOH. The diffusional cross section of MeOH is 17.6 Å^2 while that of MTBE is 40.0 Å^2. Therefore, it seems that solubility is the predominant parameter when the smaller size molecule MeOH is considered, whereas diffusion of the larger molecule MTBE impart some effects on the overall solubility at high MTBE concentration in liquid mixture. Furthermore, the extent of the mutual interactions seems to be strong near the azeotropic point where the MeOH concentration in the sorbed liquid is low (Fig. 5). For higher MeOH concentration in the liquid mixture, mutual interactions between MeOH and MTBE becomes weaker and interactions between MeOH and membrane become predominant. Therefore, MeOH molecules replace the MTBE ones inside the membrane polymer chain and, consequently, the MeOH concentration in the sorbed liquid increases.

From the overall solubility, the preferential sorption of the binary liquid mixture MeOH/MTBE into the membranes can be described by the following expression, which has been derived from the Flory–Huggins thermodynamics [30].

$$\ln\left(\frac{\varphi_1}{\varphi_2}\right) - \ln\left(\frac{v_1}{v_2}\right) = (l-1)\ln\left(\frac{\varphi_2}{v_2}\right) - g_{12}[(v_1 - v_2) + (\varphi_2 - \varphi_1)] - \varphi_3(\chi_{13} - l\chi_{23}) \quad (6)$$

where the indexes 1 and 2 refer to the binary liquid components (1 for MeOH and 2 for MTBE) and index 3 refers to the polymer membrane; v_i represents the volume fraction of liquid i in the binary liquid mixture; l is the ratio of molar volume fractions of MeOH and MTBE (i.e. v_1/v_2) and the volume fraction of component i in the ternary polymeric phase is denoted by φ_i ($\varphi_1+\varphi_2+\varphi_3=1$). The binary interaction parameters between MeOH and the polymer (χ_{13}) and between MTBE and the polymer (χ_{23}) were assumed to be concentration independent and were calculated from the single liquid sorption data using the following expression in the case of equilibrium sorption of pure solvent in a polymer [30].

$$\chi_{i3} = \frac{-\ln \varphi_i - \varphi_3}{\varphi_3} \quad (7)$$

Table 5
Overall solubility (S) and volume fractions of methanol (u_1) and MTBE (u_2) in the liquid sorbed in the membranes (PPO and filled PPO membranes: SPPO1, SPPO2, MSPPO1 and MSPPO2) at 25 °C as a function of methanol weight fraction in feed liquid mixture

MeOH in feed (wt%)	PPO	SPPO1	SPPO2	MSPPO1	MSPPO2
S (%)					
0	12.12	9.09	10.35	12.50	10.00
15.9	15.14	13.46	16.67	16.07	16.13
26.3	17.19	17.74	19.70	17.74	19.23
51.7	17.74	20.83	20.46	19.05	20.00
76.2	19.35	20.37	20.97	21.15	21.43
90.6	18.75	18.18	20.31	20.83	21.88
100	19.35	20.83	21.21	22.50	23.08
$u_1 = \varphi_1/(\varphi_1 + \varphi_2)$					
0	0	0	0	0	0
15.9	0.43	0.39	0.38	0.42	0.38
26.3	0.50	0.43	0.44	0.49	0.44
51.7	0.61	0.52	0.55	0.60	0.54
76.2	0.71	0.64	0.66	0.70	0.65
90.6	0.83	0.78	0.79	0.82	0.78
100	1	1	1	1	1
$u_2 = \varphi_2/(\varphi_1 + \varphi_2)$					
0	1	1	1	1	1
15.9	0.57	0.61	0.62	0.58	0.62
26.3	0.50	0.57	0.56	0.51	0.56
51.7	0.39	0.48	0.45	0.40	0.46
76.2	0.29	0.36	0.34	0.30	0.35
90.6	0.17	0.22	0.21	0.18	0.22
100	0	0	0	0	0

where φ_i is the volume fraction of the solvent (1 for MeOH and 2 for MTBE) in the polymer, and φ_3 is the volume fraction of the polymer. The calculated values χ_{13} (for MeOH) were smaller than χ_{23} (for MTBE). As the affinity or interaction between the polymer and the penetrants increases, the amount of liquid inside the polymer increases and χ_{i3} decreases. This indicates that MeOH is more soluble than MTBE in both PPO and filled PPO membranes.

The binary interaction parameter, g_{12}, between MeOH and MTBE was calculated from the following equation [30].

$$g_{12} = \frac{1}{x_1 u}\left[x_1 \ln\left(\frac{x_1}{u_1}\right) + x_2 \ln\left(\frac{x_2}{u_2}\right) + \frac{\Delta G^{E}}{RT}\right] \quad (8)$$

where x_1 and x_2 are the mole fractions of MeOH and MTBE in the mixture, respectively, and the excess free energy of mixing, ΔG^{E}, of the system MeOH/MTBE has been calculated using the data given elsewhere [31].

Finally, from Eqs. (6)–(8), the composition of the sorbed liquid in each membrane can be determined. The volume fraction of MeOH in the liquid mixture sorbed in the membrane, $u_1 = \varphi_1/(\varphi_1 + \varphi_2)$, and the volume fraction of MTBE in the liquid mixture sorbed in the membrane, $u_2 = \varphi_2/(\varphi_1 + \varphi_2)$, were calculated for each liquid mixture and for each membrane. The results are also given in Table 5. It can be seen that u_1 increases with the concentration of MeOH in feed, while u_2 decreases. For MeOH/MTBE liquid mixture higher than 26.3 wt%, MeOH content in the sorbed liquid (u_1) becomes higher than that of MTBE (u_2). This is in accordance with the discussions stated previously in this section.

3.5. Pervaporation experiments

Fig. 3 shows the total permeation flux at 25 °C of both unfilled PPO and filled PPO membranes as a function of the MeOH concentration in the feed mixture. With increasing MeOH concentration in the feed solution, the total permeation flux of all membranes increases. According to the swelling experiments (Table 5), the overall solubility of the membranes increased with the increase in MeOH concentration. Therefore, it may be stated that the overall solubility is the responsible of the increase in the permeation flux. Compared to the permeation flux of PPO membrane, the fluxes of all filled PPO membranes are lower. It can be seen that the permeation flux of the filled PPO membranes

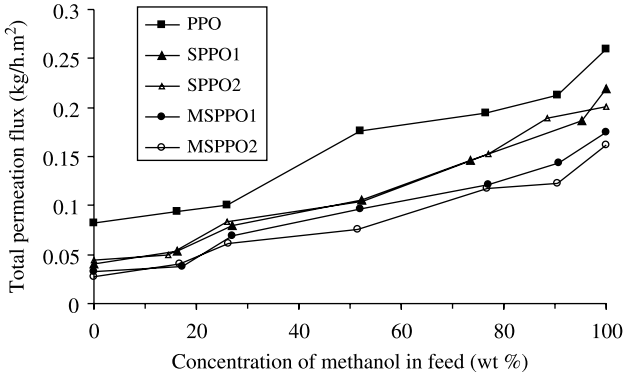

Fig. 3. Pervaporation flux of PPO and filled PPO membranes (SPPO1, SPPO2, MSPPO1, MSPPO2) at 25 °C as a function of the concentration of methanol in the feed liquid mixture.

with silane modified silica is lower than that of silica filled PPO membranes, especially at high MeOH concentration in feed mixture. Because the overall solubilities of the filled PPO membranes are similar, the low permeation flux observed for the filled PPO membranes with silane modified silica may be attributed to the higher potential of silane modified silica nanoparticles to be dispersed in PPO polymer, as explained earlier, generating in this case more tortuous pathways throughout the thickness of these membranes than in the unmodified silica filled PPO membranes. Consequently, the diffusion of both MeOH and MTBE in the filled PPO membranes with silane modified silica should be smaller than in the unfilled PPO and in the filled PPO membrane with silica.

The flux of MeOH and MTBE were calculated from the composition of the permeate. The results are plotted in Fig. 4(a) and (b) as function of MeOH concentration in the feed. The MeOH permeation flux is much higher than that of MTBE for all membranes. This may be attributed in part to the preferential sorption of MeOH molecules in both PPO and filled PPO membranes. In addition, the behavior of the MTBE permeation flux is different from that of the MeOH one. The permeation flux of MeOH increases with MeOH concentration in the feed while that of MTBE decreases. In comparison to the PPO membrane, the filled membranes exhibit lower MeOH flux (up to 44.3% for MSPPO2 membrane) and much lower MTBE flux (up to 90.1% for MSPPO2 membrane). Again, it can be seen lower MeOH and MTBE fluxes for the filled PPO membranes with modified silica than the corresponding fluxes of the filled PPO membrane with the unmodified silica nanoparticles.

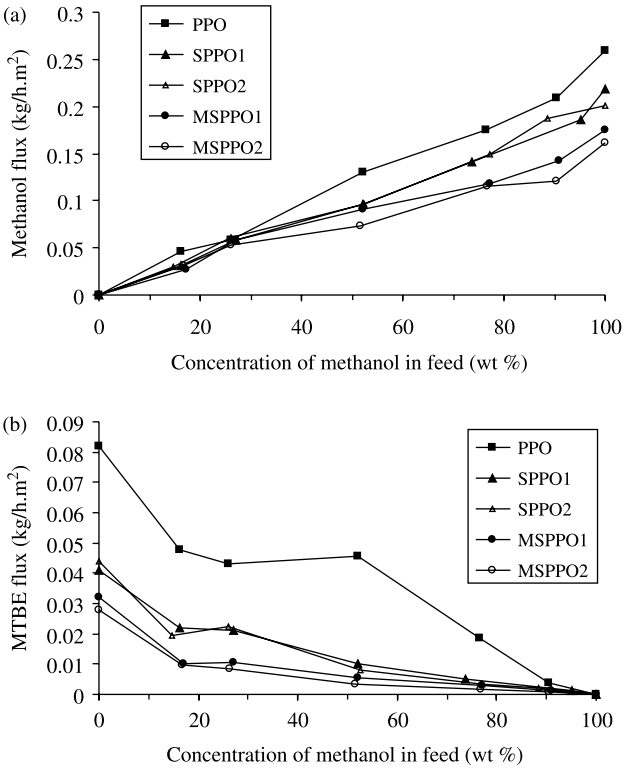

Fig. 4. Methanol (a) and MTBE (b) permeation flux of PPO and filled PPO membranes (SPPO1, SPPO2, MSPPO1, MSPPO2) at 25 °C as a function of the concentration of methanol in the feed liquid mixture.

Fig. 5 presents the separation performance of PPO, silica filled PPO and silane modified silica filled membranes, at 25 °C, where the concentration of MeOH in permeate obtained in the PV experiments has been plotted against the concentration of MeOH in the feed mixture. The vapor–liquid equilibrium diagram (VLE) and the variation of MeOH concentration of the sorbed liquid in PPO membrane (i.e. MeOH sorption curve), with MeOH feed concentration, are also shown for comparison [31]. From this figure, it is clear that all the tested membranes are MeOH selective and the PV permeate/feed compositions diagram is different from the VLE diagram of MeOH/MTBE mixture. The MeOH selectivity of PV is higher than that of the distillation, indicating a greater separation potential of PV. This demonstrates the relative merits of PV against distillation of MeOH/MTBE mixtures. The membrane permeates MeOH preferentially and the MeOH concentration in the permeate overcomes the azeotropic limitation of distillation. Furthermore, the PV feed-permeate composition lines are above the sorption line of PPO taken as reference. This may be due to much greater diffusion of the much smaller size molecule, MeOH, through the membranes. This fact puts in evidence also the important role of diffusion through the PPO and filled PPO membranes.

At MeOH feed concentration higher than 50 wt%, the MeOH concentration in permeate is almost the same for all filled PPO membranes. However, at MeOH concentration values in feed mixture lower than 50 wt%, permeation selectivity for MeOH follows the trend: MSPPO2 > MSPPO1 > SPPO2 > SPPO1 > PPO. From the overall solubility and the preferential sorption results summarized in Table 5, no clear tendency was observed between these membranes indicating that silica and silane modified silica nanoparticles affect predominantly diffusion selectivity since permeation in PV is a combination of both sorption and diffusion. It must be stated that there is no significant increase in the permeate MeOH concentration when the concentration of silica or silane modified silica in filled PPO membranes was increased from 5 to 10 wt%.

From the MeOH and MTBE permeation fluxes and the sorption data reported in Table 5, the diffusion coefficients of both MeOH and MTBE were determined by using the theoretical approach reported elsewhere [32] and summarized in Appendix A. A numerical analysis of the experimental fluxes and sorption data given in Table 5 was carried out. Table 6 shows the diffusion coefficients of MeOH and MTBE through the membranes at infinite dilution. For all considered membranes, the diffusion coefficient of MeOH is much higher than that of MTBE. In fact, the relative diffusion depends mainly on the

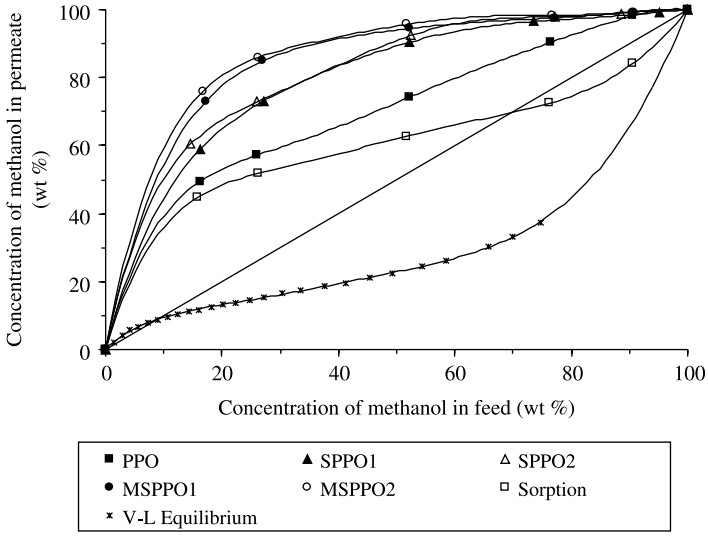

Fig. 5. Variation of the concentration of methanol in the permeate and in the membrane with its feed concentration of methanol in the mixture at 25 °C.

diffusional cross section of the permeants, which is smaller for MeOH. The diffusion of both MeOH and MTBE decreases following the order: PPO > SPPO1 > SPPO2 > MSPPO1 > MSPPO2. The lower diffusion coefficients of the PPO membranes filled with silane modified silica nanoparticles may be attributed to the fact that the silane modified silica is more compatible with PPO polymer than the unmodified silica and the latter nanoparticles are better dispersed throughout the PPO membrane matrix creating more tortuous path for the passage of both MeOH and MTBE. On the other hand, a possible reaction may take place between silanol superficial groups of the silica forming ethoxy groups by elimination of water. This effect seems to be minor compared to that of the diffusion as MeOH selectivity is higher than that of the unfilled PPO membrane. In addition, the diffusion selectivity of MeOH was also calculated from the ratio of the diffusion coefficients of MeOH and MTBE. The results are also given in Table 6. It was found that MeOH selectivity at infinite dilution follows the same order given previously for permeation selectivity when MeOH concentration in feed mixture is lower than 50 wt% (MSPPO2 > MSPPO1 > SPPO2 > SPPO1 > PPO). This confirms that the fillers silica and silane modified silica nanoparticles affect predominantly diffusion selectivity.

Table 6
Diffusion coefficients of MeOH ($D_{0,1}$) and MTBE ($D_{0,2}$) and diffusion selectivity of MeOH ($D_{0,1}/D_{0,2}$) of all membranes at infinite dilution

Membrane	$D_{0,1}$ (10^{-12} m^2/s)	$D_{0,2}$ (10^{-13} m^2/s)	$D_{0,1}/D_{0,2}$
PPO	1.98	6.56	3.02
SPPO1	1.76	3.19	5.53
SPPO2	1.64	3.12	5.24
MSPPO1	1.37	2.27	6.03
MSPPO2	1.35	2.06	6.55

4. Conclusions

The surface modification of the hydrophilic inorganic silica nanoparticles with organosilanes reduces the number of the superficial silanol groups, and grafts molecules with organic nature forming silane stable network on silica surface. This was investigated by means of contact angles and environmental scanning electron microscopy (ESEM).

The X-ray diffraction spectra and the mechanical strength of the unfilled and the filled poly(2,6-dimethyl-1,4-phenylene oxide) (PPO) dense membrane with silica and silane modified silica nanoparticles were found to be similar, whereas the filled PPO membranes exhibit higher decomposition temperature than the unfilled PPO membranes.

The overall solubility, increases with the increase in methanol concentration in methanol/methyl *tert* butyl ether (MTBE) mixture. This overall solubility is slightly lower for the unfilled PPO membranes and similar for all the filled membranes.

All filled and unfilled PPO membranes exhibit greater affinity to methanol than to MTBE and are methanol selective when pervaporation experiments are performed using methanol/MTBE mixtures. However, the methanol selectivity is higher for the filled PPO membranes with silane modified silica, followed by that of the filled PPO membrane with the unmodified silica and then the unfilled PPO membrane. This was attributed mainly to the predominant effect of the diffusion over sorption effect, which was found to be practically the same for all membranes.

The modified silica nanoparticles have stronger affinity and enhanced compatibility with PPO polymer than the unmodified silica nanoparticles. This generates more tortuous pathways in PPO dense membrane matrix, reduces the diffusion of both methanol and MTBE, and consequently the pervaporation permeation flux decreases.

Acknowledgements

The authors of this study gratefully acknowledge the financial support of the Ministry of Science and Technology (MCYT, Spain) through its project No PPQ2003-03299. Dr López-Manchado also acknowledges the concession of a Ramón and Cajal contract from the MCYT.

Appendix A

Mass transfer through a dense membrane in pervaporation occurs by a solution–diffusion mechanism. The permeants interact with the membrane as well as with each other. The permeate flux of the component i is given by Fick's first law as [32]:

$$J_i = -\rho_m D_i \frac{dw_{im}}{dL} \quad (A.1)$$

where ρ_m is the membrane density, D_i is the diffusion coefficient of the component i, w_{im} is the membrane phase mass fraction of the component i and L is the membrane thickness.

The diffusion coefficient is not constant along the membrane thickness and depends on temperature, concentration of the permeants components and their mutual coupling effect. Assuming a constant temperature, the diffusion coefficient for the component i can be described by Eq. (A.2) as reported in [32]:

$$D_i = D_{i0} \exp(w_{im} + \sigma w_{jm}) \quad (A.2)$$

where D_{i0} is the diffusion coefficient of i at infinite dilution, w_{jm} is the membrane phase mass fraction of the component j and σ is the plastization factor for component j.

By substituting Eq. (A.2) in Eq. (A.1) and integrating over the membrane thickness yields to:

$$\int_0^L J_i dL = -\rho_m D_{i0} \int_{w_{imf}}^{w_{imp}} \exp(w_{im} + \sigma w_{jm}) dw_{im} \quad (A.3)$$

where w_{imf} and w_{imp} are the membrane phase mass fraction at feed and permeate side, respectively.

The concentration of the permeating components on the downstream side may be considered zero due to the very low pressure, and thus Eq. (A.3) for the ith component reduces to:

$$J_i = \frac{\rho_m D_{i0}}{L} [\exp(w_{imf} + \sigma w_{jmf}) - 1] \quad (A.4)$$

Similar procedure may be used to determine the flux of the jth component:

$$J_j = \frac{\rho_m D_{j0}}{L} [\exp(w_{jmf} + \mu w_{imf}) - 1] \quad (A.5)$$

where μ is the plastization factor for component i.

From the obtained permeation fluxes, J_i and J_j, and the sorption data given in Table 5 a numerical analysis was carried out to determine D_{i0} and D_{j0}.

References

[1] Moaddeb M, Koros WJ. J Membr Sci 1997;125:143–63.
[2] Chen X, Ping ZH, Long YC. J Appl Polym Sci 1998;67:629–36.
[3] Bottino A, Capannelli G, D'Asti V, Piaggio P. Sep Purif Techol 2001; 22:26–275.
[4] Genné I, Doyen W, Adriansens W, Leysen R. Filtr Sep 1997;34: 964–6.
[5] Goosens I, Van Haute A. Desalination 1976;18:203–14.
[6] Kumar S, Shah JN, Sawant SB, Joshi JB, Pangarkar VG. J Membr Sci 1997;134:225–33.
[7] Nunes SP, Ruffmann B, Rikowski E, Vetter S, Richau KJ. Membr Sci 2002;203:215–25.
[8] Nunes SP, Peinemann KV, Ohlrogge K, Alpers A, Keller M, Pires ATN. J Membr Sci 1999;157:219–26.
[9] Chowdhury G, Kruczek B, Matsuura T. Polyphenylene oxide and modified polyphenylene oxide membranes: gas, vapor and liquid separation. 1st ed. Dordrecht, The Netherlands: Kluwer Academic; 2001.
[10] Doghieri F, Nardella A, Sarti GC, Valentín C. J Membr Sci 1994;91: 283–91.
[11] Khayet M, Villaluenga JPG, Godino MP, Mengual JI, Seoane B, Khulbe KC, Matsuura T. J Colloid Interf Sci 2004;278:410–22.
[12] Villaluenga JPG, Godino P, Khayet M, Seoane B, Mengual JI. Ind Eng Chem Res 2004;43:2548–55.
[13] Chen MS, Eng RM, Glazer JL, Wensley CG. US Patent; 1988.
[14] Park HC, Ramaker NE, Mulder MHV, Smolders CA. Sep Sci Technol 1995;30:419–33.
[15] Sano T, Hasegawa M, Kawakami Y, Yanagishita H. J Membr Sci 1995;107:197–8.
[16] Chen WJ, Martin CR. J Membr Sci 1995;104:101–8.
[17] Zhou M, Persin M, Sarrazin J. J Membr Sci 1996;117:303–9.
[18] Nam SY, Lee YM. J Membr Sci 1997;135:161–71.
[19] Cao S, Shi Y, Chen G. J Appl Polym Sci 1999;71:377–86.
[20] Yoshikawa M, Yoshioka T, Fujime J, Murakami A. J Membr Sci 2000;178:75–8.
[21] Kim SG, Lim GT, Jegal J, Lee KH. J Membr Sci 2000;174:1–15.
[22] Bangxiao C, Li Y, Hailin Y, Congjie G. J Membr Sci 2001;194:151–6.
[23] Villaluenga JPG, Khayet M, Godino P, Seoane B, Mengual JI. Ind Eng Chem Res 2003;42:386–91.
[24] Wijmans JG, Rutten HJJ, Smolders CA. J Polym Sci Phys Ed 1985;23: 1941–55.
[25] Khulbe KC, Matsuura T, Lamarche G, Lamarche AM. J Membr Sci 2000;170:81–9.
[26] Van Oss CJ, Chaudhury MK, Good R. J Adv Colloid Interf Sci 1987; 28:35–64.
[27] Van Oss CJ, Chaudhury MK, Good R. J Chem Rev 1988;88:927–41.
[28] Khayet M, Chowdhury G, Matsuura T. AIChE J 2002;48:2833–43.
[29] Mandal S, Pangarkar VG. J Membr Sci 2002;201:175–90.
[30] Huang RYM. Pervaporation membrane separation processes. 1st ed. Membrane science and technology series. vol. 1. New York: Elsevier Science; 1991.
[31] Coto B, Wiesenberg R, Pando C, Rubio RG, Renuncio JAR. Ber Bunsenges Phys Chem 1996;100:482–9.
[32] Bhat AA, Pangarkar VG. J Membr Sci 2000;167:187–201.